

## TEMPERATURE GRADIENT MEASUREMENTS IN COMBUSTION DROPLETS BY STANDARD RAINBOW THERMOMETRY

M. R. Vetrano\*, J. van Beeck\* and M. Riethmuller\*

\* Environmental and Applied Fluid Dynamic department  
Von Karman Institute for Fluid Dynamics, B-1640 Rhode-saint-Genèse, Belgium

### ABSTRACT

Standard Rainbow Thermometry is a non-intrusive laser based technique used to measure the refractive index and the size of transparent particles immersed in a transparent environment possessing a lower refractive index as for a spray. The refractive index and size determination are based on the analysis of the interference fringes pattern generated by the interaction of monochromatic laser light, linearly polarized, and the particles themselves using the Airy theory. In this paper first some problems of the Airy theory, as a bow spacing modification and a non-linear increment in the intensity respect to the Lorenz-Mie patterns, will be presented. Using correction functions, these two problems will be overcome for a large range of particle size. Then a data inversion algorithm that can be used to determine with a good precision the diameter and the refractive index at the core and at the surface of a droplet presenting an internal profile of refractive index will be presented. This data inversion algorithm will be tested on the case of an n-octane droplet burning in a standard atmosphere.

### INTRODUCTION

The most complete and rigorous approach to the problem of monochromatic light scattering by a transparent sphere is due to Lorenz and Mie [1]. Mie theory is named after its developer German physicist Gustav Mie (1868-1957) and Danish physicist Ludvig Lorenz (1829-1891) who independently developed the theory of electromagnetic plane wave scattering by a dielectric sphere in 1908. In the same period Petrus Josephus Wilhelmus Debye, known as Peter Debye (1884-1966) solved the problem of plane wave scattering by a cylinder that can be easily adapted to scattering by a sphere [2], the advantage of the Debye approach is the possibility to isolate the contribution of the internal and external waves to the diffraction, the transmission, the primary and the secondary rainbow. The Complex Angular Momentum (CAM) theory has been developed by Herch Nussenzveig starting from the Debye approach [3], [4]. The CAM theory, using some approximations relative to the scattering region taken into account, writes the Debye series into integrals that have analytical solution. This approach has the advantage to be very low time consuming respect to the Lorenz-Mie or Debye theory, but it needs heavy mathematics.

A totally different approach to the scattering phenomenon is the one of Airy. The Airy theory for light scattering by small spheres can be seen as a hybrid approach. Indeed first it uses the Descartes law, i. e. the geometric optics, in order to graphically find the wave front of the scattered wave. Then it applies the Huygens-Fresnel principle to get the light intensity in the observation point. This approach has the great advantage to be of very simple implementation and no time consuming. On the other hand it presents a non linear harmonic shift in the scattering angle and a non linear overestimation of the bows intensity respect to the Lorenz-Mie pattern.

In a previous work of the authors [5] the Airy theory has been extended to inhomogeneous spheres using a generalized form of the Descartes law. This theory allows the computation of the light scattering intensity of a sphere possessing a continuous refractive index gradient giving then the possibility to extend the Airy approach to physical phenomenon as droplet combustion or diffusion.

The goal of this paper is to show how, for a limited range of sphere diameter it is possible to find empirical laws that minimize the discrepancies between Airy and Lorenz-Mie patterns both for the homogeneous and the inhomogeneous case.

### COMPARISON BETWEEN RAINBOW THEORIES

In this paragraph a short description of the mathematical formulations of the Lorenz-Mie, Debye and Airy theory will be given. It is out of the scope of this manuscript to give a full description of these theories; the reader will find a more exhaustive work in the reference [6]. The light scattering intensity patterns obtained from these theories will be compared in order to find out the main source of discrepancies between them.

### Lorenz-Mie theory for homogeneous and inhomogeneous spherical particles.

A rigorous theoretical approach to the rainbow phenomenon requires the calculation of the electromagnetic field of the light scattered by a homogeneous sphere of arbitrary size. This means to solve the complete set of Maxwell equations with opportune boundary conditions. It can be proved that in this case the light scattered intensity by a plane waves can be written as follows (Figure 1):

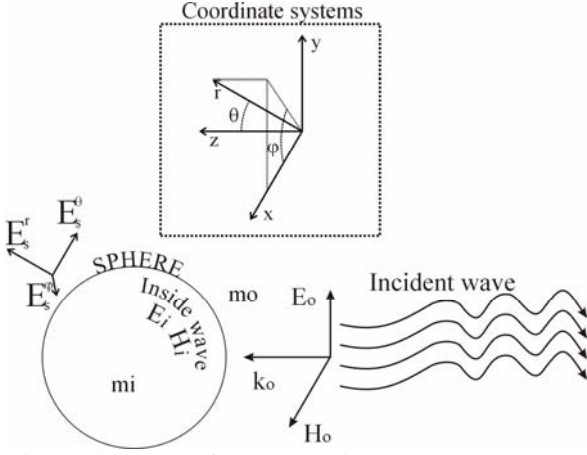


Figure 1 Sketch of the scattering problem

$$I(\theta, \varphi, r) = \left[ |S_1(\theta)|^2 \sin^2(\varphi) + |S_2(\theta)|^2 \cos^2(\varphi) \right] \frac{I_i}{k r} \quad (1)$$

$$\begin{aligned} |S_1(\theta)|^2 &= \sum_{n=1}^{\infty} \frac{2n+1}{n(n+1)} \left[ a_n \cdot \frac{\pi_n \cos(\theta)}{\tau_n \cos(\theta)} + b_n \cdot \frac{\tau_n \cos(\theta)}{\pi_n \cos(\theta)} \right] \\ |S_2(\theta)|^2 & \end{aligned} \quad (2)$$

Where  $I_i$  is the intensity of the incident light,  $k$  is the amplitude of the wave vector,  $\pi_n \cos(\theta)$  and  $\tau_n \cos(\theta)$  are functions of the associated Legendre polynomial  $P_n^1(\cos \theta)$

$$\pi_n(\cos \theta) = \frac{P_n^1(\cos \theta)}{\sin \theta}$$

$$\tau_n(\cos \theta) = \frac{d}{d\theta} P_n^1(\cos \theta)$$

(3)

The coefficient  $a_n$  and  $b_n$  are function of the Riccati-Bessel functions  $\psi_n(\rho)$ ,  $\xi_n(\rho)$ :

$$a_n = \frac{\psi_n'(y)\psi_n(x) - m\psi_n(y)\psi_n'(x)}{\psi_n'(y)\xi_n(x) - m\psi_n(y)\xi_n'(x)} \quad (4)$$

$$b_n = \frac{m\psi_n'(y)\psi_n(x) - \psi_n(y)\psi_n'(x)}{m\psi_n'(y)\xi_n(x) - \psi_n(y)\xi_n'(x)}$$

where  $x=2\pi a/\lambda$ ,  $y=mka$ ,  $m$  is the relative sphere refractive index,  $a$  is the sphere radius and  $\lambda$  is the light wavelength.

The generalization of the Lorenz-Mie Theory to non-homogeneous spheres [7] is obtained dividing the sphere in a fixed number of concentric layers and using opportune boundary conditions between the sphere layers in order to find the coefficients  $a_n$  and  $b_n$ .

## Debye theory

The Debye mathematical formulation of the scattering problem follows the lines of the Lorenz-Mie one. The main difference consists in the fact that the contributions of any term of the scattered waves can be distinguished. Defining  $p$  as the number of light reflection inside the sphere it is possible to distinguish the diffraction ( $p=0$ ), the transmission ( $p=1$ ), primary ( $p=2$ ) and secondary ( $p=3$ ) rainbow.

The differentiation between the different terms of the scattered wave is done associating to these ones transmission  $T^{ij}$  and reflection  $R^{ij}$  coefficients as in geometric optics (Figure 2).

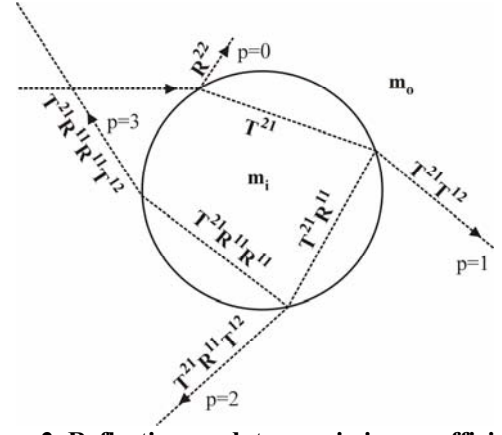


Figure 2 Reflection and transmission coefficients for the internal and external waves generated according to Debye. The use of rays has been used only for seek of simplicity.

Consequently the coefficients  $a_n$  for TM amplitudes and  $b_n$  for TE amplitudes are written as :

$$z_n(x, y) = 0.5 \left[ 1 - R_n^{22}(x, y) - G_n(x, y) \right] \quad (5)$$

$$G_n(x, y) = \sum_{p=1}^{\infty} T_n^{21}(x, y) \left( R_n^{11}(x, y) \right)^{p-1} T_n^{12}(x, y)$$

where

$$T_n^{21}(x, y) = - \left( \frac{n_1}{n_n} \right) \frac{2i}{D_n(x, y)} \quad (6)$$

$$T_n^{12}(x, y) = - \frac{2i}{D_n(x, y)} \quad (7)$$

$$R_n^{22}(x, y) = \frac{[\alpha h_n^{(2)}(x)h_n^{(2)}(y) - \beta h_n^{(2)}(x)h_n^{(2)}(y)]}{D_n(x, y)} \quad (8)$$

$$R_n^{11}(x, y) = \frac{[\alpha h_n^{(1)}(x)h_n^{(1)}(y) - \beta h_n^{(1)}(x)h_n^{(1)}(y)]}{D_n(x, y)} \quad (9)$$

$$D_n(x, y) = -\alpha h_n^{(1)}(x)h_n^{(2)}(y) + \beta h_n^{(1)}(x)h_n^{(2)}(y) \quad (9)$$

The quantity  $x$  and  $y$  have been expressed in the previous paragraph and  $\alpha$  and  $\beta$  are defined for TE and TM waves as it follows :

$$\text{TE} : \alpha = 1, \quad \beta = m; \quad (10)$$

$$\text{TM} : \beta = m, \quad \alpha = 1$$

## Airy Theory for homogeneous and inhomogeneous spherical particles.

The intensity of the light scattered by a droplets with diameter  $D$  and relative refractive index  $m$  illuminated by a monochromatic light of wavelength  $\lambda$ , in the Airy theory, can be written as :

$$I \propto \left| \Omega(z) \right|^2 = \left| \int_0^{\infty} \cos \left[ \frac{1}{2} \pi \left( (z[D, \lambda, m]) \eta - \eta^3 \right) \right] d\eta \right|^2 \quad (11)$$

where

$$\eta = v \left( \frac{4h}{\lambda D^2} \right)^{1/3} \quad (12)$$

$$z[\theta, D, \lambda, m] = -(\theta - \theta_{rg}[m]) \left(\frac{16}{h}\right)^{1/3} \left(\frac{D}{\lambda}\right)^{2/3} \quad (13)$$

In Eq. 12 the quantity  $v$  represent the ordinate of the Cartesian coordinate system used for the light scattered wavefront (Figure 3),  $\theta$  is the scattering angle and  $h$  is defined as follows:

$$h = \frac{2}{3} \frac{\partial^2 \theta}{\partial \tau^2} \bigg|_{\tau=\tau_{rg}} \frac{1}{\sin^2 \tau_{rg}} \quad (14)$$

$\tau_{rg}$  and  $\theta_{rg}$  represents the coordinates of the minimum of the function :

$$\theta[\tau] = 2\tau - 2(p) \cdot \arcsin\left(\frac{\sin \tau}{m}\right) \quad (15)$$

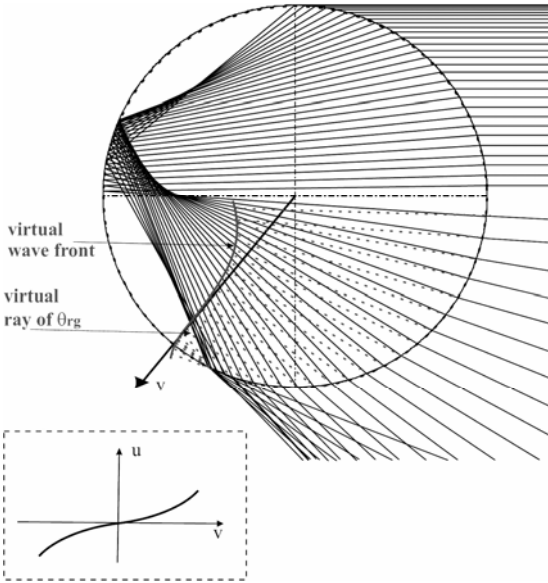


**Figure 3** Drawing of the virtual scattered wavefront generated by a spherical particle with a relative refractive index equal to 1.33.

The generalization of the Airy theory to non homogeneous spheres (GAT theory) [8], is obtained generalizing Eq. 15 to spherically symmetric refractive indexes  $m[r]$

$$\theta[\tau, \tilde{r}] = 2\tau - 2(p) \cdot \chi_1[\tau, \tilde{r}], \quad (16)$$

where  $\chi_1$  is can be found by integrating the differential equation of the light rays inside the sphere:

$$\chi_1[\tau, \tilde{r}] = \int_{\tilde{r}_m}^{\tilde{r}} \frac{m_e \cos \tau}{r \sqrt{m[\tilde{r}]^2 \tilde{r}^2 - (m_e \cos \tau)^2}} \partial \tilde{r}, \quad (17)$$

where  $m_e$  the refractive index of the sphere environment,  $\tilde{r} = r/R$  the non-dimensional sphere radius and  $\tilde{r}_m$  representing the minimal distance of the light ray from the center of the sphere.

### Patterns comparison

In Figure 4 the rainbow patterns for obtained using the Lorenz-Mie, the Debye and the Airy theory are shown. In particular for the Debye and the Airy pattern the differentiation between the primary ( $p=2$ ) and the secondary ( $p=3$ ) rainbow is made. The patterns have been all calculated for a sphere of 60  $\mu\text{m}$  of diameter. The impacting plane wave is perpendicular polarized and has a wavelength of  $\lambda=0.5145 \mu\text{m}$  corresponding to one of the green wavelength in an

argon-ion laser. The relative refractive index of the sphere respect to its environment is set to  $m=1.330$ .

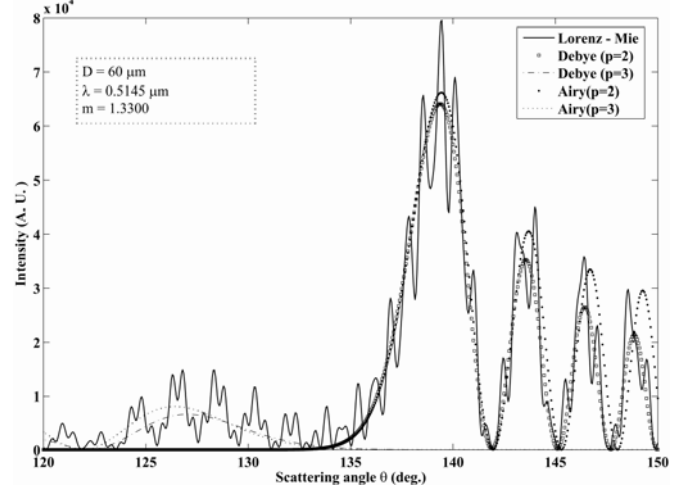


**Figure 4.** Rainbow profiles for a sphere of 60  $\mu\text{m}$  diameter, possessing a relative refractive index of  $m=1.3300$  and illuminated by a plane wave perpendicularly polarized ( $\lambda=514.5 \text{ nm}$ ) according to the Lorenz-Mie, the Debye and the Airy theories

The first difference in the patterns consists in the fact that the Lorenz-Mie pattern is composed by the primary and the secondary rainbow, while the Debye and Airy theories compute them separately. Figure 1 shows a bow space modification in the Airy pattern respect to the Lorenz-Mie and the Debye ones. This one is clearly visible starting from the third bow, moreover a non linear overestimation of the bows intensities is also present. The Lorenz-Mie pattern (solid line of Figure 4) presents an additional structure superimposed to the main one.

This structure is called ripple structure and it is due to the contribution of the surface rays and the purely reflected rays to the far field interference image. The frequency of the ripple structure decreases with the droplet size, approaching for small droplets ( $D \sim 30 \text{ nm}$ ) the frequency of the bows. This behaviour of the ripple structure becomes a problem when the ripple structure covers the main rainbow maximum rendering very difficult the angular analysis of the signal itself.

Moreover the choice to filter the LM signal in order to get rid of the ripple structure can be dangerous when the ripple structure becomes of such importance (see Figure 5).

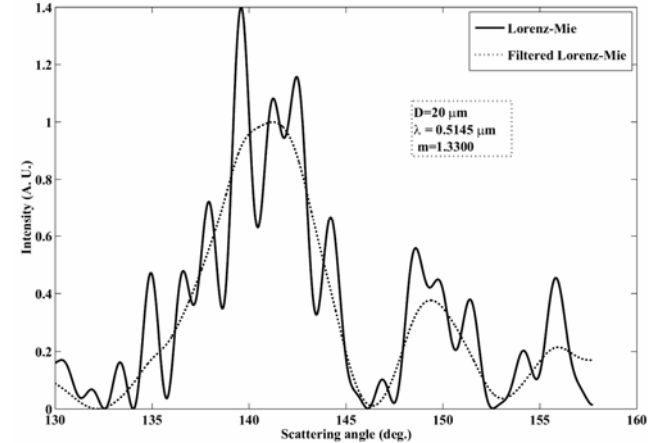


**Figure 5** Comparison between the Lorenz-Mie pattern for a droplet of 20  $\mu\text{m}$  of diameter and the same signal filtered with a low pass filter for ripple removal. The light wavelength is  $\lambda=514.5 \text{ nm}$  and the refractive index is  $m=1.330$ .

The filtered pattern (solid line) is deformed by the filtering and this is due to the fact that the ripple and the main rainbow frequencies are very close as it is possible to see from Figure 6.

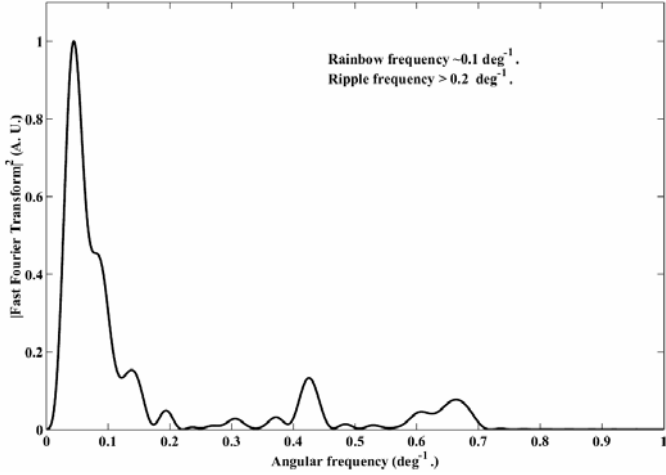


**Figure 6 Spectral frequency of the Lorenz-Mie pattern of a sphere of 20  $\mu\text{m}$  of diameter possessing a relative refractive index of  $m=1.330$  and illuminated by a planar wave with wavelength of  $\lambda=514.5 \text{ nm}$ .**

The Debye pattern is more consistent with the Lorenz-Mie one. Debye patterns approximate very well the Lorenz Mie filtered one also for small values of droplet diameter.

Figure 7 shows the comparison between the Lorenz-Mie and the GAT scattering intensity profile for a sphere possessing a diameter  $D=100 \mu\text{m}$ , a parabolic refractive index

$$m[r] = m_c - 4(m_c - m_s) \frac{r^2}{D^2} \quad (18)$$

and illuminated by a plane wave possessing a wavelength of  $\lambda=0.5145 \mu\text{m}$ .

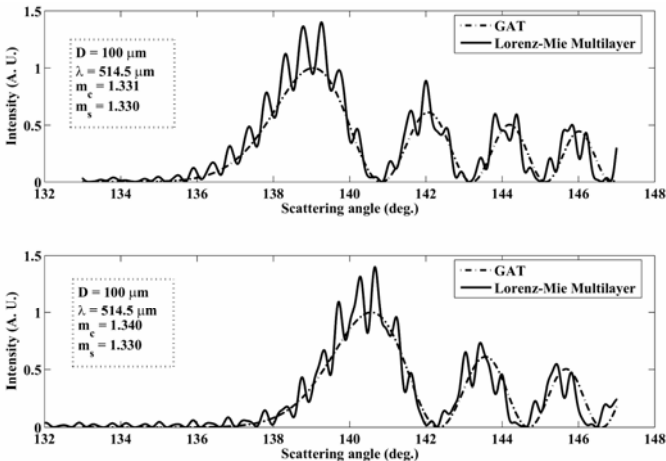


**Figure 7 Comparison between the Lorenz-Mie multilayer theory and the Generalized Airy theory for a spherical particle with parabolic internal refractive index gradient.**

In both the plots of Figure 7 the refractive index profiles are parabolic and 2000 layers have been adopted for the Lorenz-Mie multilayered case. The two plots differs mainly in the size of the refractive index gradient,  $\Delta m=0.001$  for the first plot and  $\Delta m=0.01$  for the second one. For both the plots, as in the homogeneous case, the GAT patterns agree well the Lorenz-Mie ones but the angular shift and the intensity overestimation are clearly visible.

## AIRY THEORY CORRECTION

As it has been shown on Figure 4, the problems encountered using the Airy theory consist in a bow spacing modification and a non-linear increment in the intensity respect to the Lorenz-Mie and Debye patterns. In this section using numerical correction functions these two problems will be overcome for sphere size ranging from 20 to 300 microns up to the seventh order bow.

The following methodology will be pursued. The homogeneous case is the first taken into consideration. The non linear angular shift of the Airy patterns varies with the scattering angle and with the sphere diameter and it is possible to show that this shift depends strongly from the sphere diameter rather than the scattering angle. For this reason the two exponents of Eq. 13, that regulates the harmonic angular behavior of the Airy pattern, will be replaced by polynomials functions of the diameter  $D$ , yielding to a new expression of the scattered light intensity  $I^*[\theta, D, \lambda, m] = I[z^*[\theta, D, \lambda, m]]$ .

The non linear scattered light intensity overestimation depends strongly from the scattering angle, as  $\theta$  increases the discrepancies between the intensity values of the Airy and Debye pattern increases too. The least square fit method is used to find a non linear function of the scattering angle  $t(\theta)$  which multiplied by the Airy scattered light intensity pattern minimize its discrepancies respect to the Debye pattern.

For the inhomogeneous case the same correction factor of the homogeneous case will be tested. The corrected GAT theory will be then compared to the filtered GLMT one for high diameter values ( $D > 150 \mu\text{m}$ ). The correction factors will be then adapted in order to minimize the discrepancies between the patterns for diameter values ranging from 150  $\mu\text{m}$  to 300  $\mu\text{m}$ . The new correction factor will be then determined, these once will be used for a visual comparison between corrected GAT and GLMT for droplet size values ranging from 20  $\mu\text{m}$  to 149  $\mu\text{m}$ . No filtering of the GLMT pattern will be effectuated in order to do not corrupt the pattern.

### Homogeneous case

The correction function for the bow spacing modification ( $n_1[D]$ ) should take the intensity peak position mismatch into account. This is done by placing two coefficients presents in the non-dimensional scattering angle  $z$ . Indeed a new form of  $z$  is supposed

$$z^*[\theta, D, \lambda, m] = -(\theta - \theta_{rg}[m])^{n_1[D] + g} \left(\frac{16}{h}\right)^{1/3} \left(\frac{D}{\lambda}\right)^{n_1[D]} \quad (19)$$

where  $g$  is a constant equal to 0.3405.

Then the angular values of the first six minima of the Debye pattern ( $\theta_{\min}^{\text{Deb}}$ ) and of the Airy one ( $\theta_{\min}^{\text{Ai}}$ ) have been calculated for size value ranging from 20 to 300 microns as function of  $n_1[D]$ . The least square fit method has been used in order to minimize the quantities  $|\theta_{\min}^{\text{Deb}} - \theta_{\min}^{\text{Ai}}|$ , with the limit that :

$$\max \left| \theta_{\min}^{\text{Deb}} - \theta_{\min}^{\text{Ai}} \right| \leq 0.01 \quad (20)$$

The function  $n_1[D]$  is a fourth polynomial order expressed as follows :

$$n_1[D] = 1.325 \cdot 10^{-11} D^4 - 1.0737 \cdot 10^{-8} D^3 + 3.2750 \cdot 10^{-6} D^2 - 4.66 \cdot 10^{-4} D + 0.702 \quad (21)$$

A comparison of the Airy patterns obtained using Eqns. 11, 19 and 21 and the Debye ones shows the absence of a fringe spacing modification as it is possible to see from Figure 8. This figure visually shows the good agreement of the angular position of the patterns maxima and minima for small ( $D=20 \mu\text{m}$ ) and large ( $D=300 \mu\text{m}$ ) spheres.

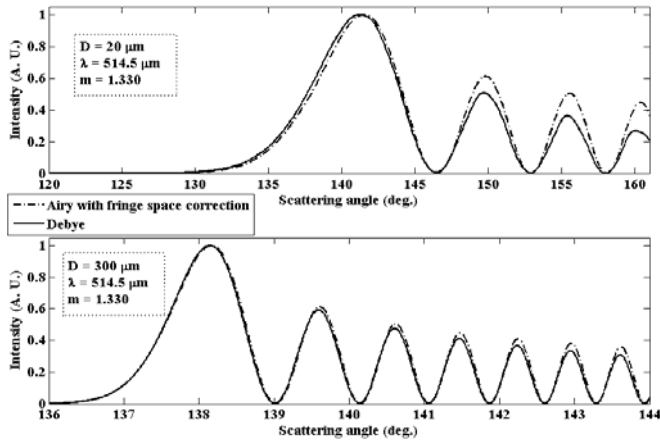


**Figure 8 Comparison between the Debye theory and the Airy one with bow modification for a spherical particle with relative refractive of 1.330 and for two different values of particle diameter.**

Eq. 21 is the result of a numerical minimization procedure performed for one single value of the light wavelength. Varying the light wavelength in the visible range one can check the independence of Eq. 21 from such a parameter. In order to give an example of that in fig. 7 the modified Airy pattern and the Debye ones are compared for different values of the wavelength. The comparison is made on small size spheres since this is the case in which a larger fringe space modification was present.

The intensity light scattered values in the Airy theory can be adjusted by means of a non linear correction function  $t[\theta]$  that is multiplied to Eq. 11. This leads to a new expression of the light scattered  $I^{**}[\theta, D, \lambda, m]$ . As for the fringe space correction, the least square fit method has been used to minimize the difference between the Debye pattern ( $I^{\text{Deb}}$ ) and the Airy pattern generated by  $I^{**}[\theta, D, \lambda, m]$ , using as fitting parameters  $t[\theta]$  and using the following condition:

$$\max \left| I^{\text{Deb}} - I^{**}[\theta, D, \lambda, m] \right| \leq 0.05 \quad (22)$$

With this condition the expression for  $t[\theta]$  is the following:

$$t[\theta] = -7.263 \cdot 10^{-9} \theta^4 + 4.431 \cdot 10^{-6} \theta^3 - 9.445 \cdot 10^{-4} \theta^2 + 5.872 \cdot 10^{-2} \theta + 1.959 \quad (23)$$

Using  $t[\theta]$  as in Eq. 23 the Airy patterns satisfactory matches the Debye one. In Figure 9 the Debye pattern obtained for a sphere of  $40 \mu\text{m}$  is compared to the modified Airy one. The discrepancies between them are minor.

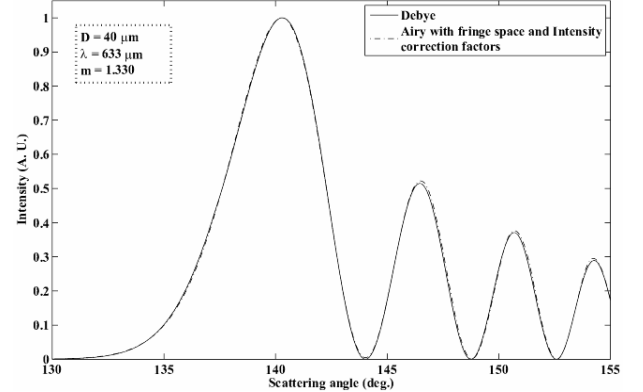


**Figure 9 Comparison between the Airy pattern obtained from  $I^{**}[\theta, D, \lambda, m]$  and the Debye pattern for a particle with relative refractive index  $m=1.330$  and diameter of  $D=40 \mu\text{m}$ .**

On Figure 10 the ratio between the corrected Airy pattern and the Debye one is plotted as function of the scattering angle and of the particle diameter. The biggest discrepancies between Airy and Debye patterns take place for small particles, diameters in the range  $[20 \mu\text{m}, 30 \mu\text{m}]$  starting from the second bow. In this case the maximum difference between the Debye and the modified Airy pattern is higher than 0.01.

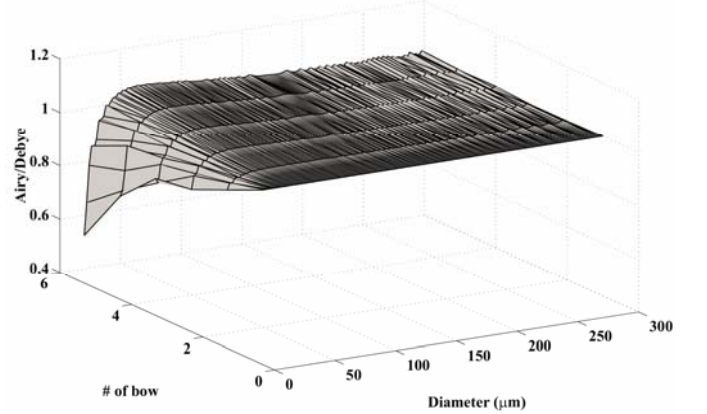


**Figure 10 Three-dimensional representation of the ratio between the corrected Airy pattern and the Debye one as function of the particle diameter and of the first six maxima of the pattern.**

Nevertheless, evaluating the error that is committed if a Debye pattern of a small droplet is inverted using a data inversion algorithm, based on the least square fit method, that uses the corrected Airy intensity function  $I^{**}[\theta, D, \lambda, m]$  one obtains the results of Tab. 1. This table shows that even for the smallest diameter the error committed for the diameter evaluation is less than 4% and that this decreases rapidly to  $\sim 1\%$ , while the same calculation made with the initial Airy

model was giving an error going from 10% to 2% in the size determination.

**Table 1 Error committed using a data inversion algorithm, based on the least square fit method, which employees the modified Airy theory to invert Debye patterns.**

D[ $\mu\text{m}$ ]	D**[ $\mu\text{m}$ ]	m	m**	$\Delta D$ %	$\Delta m$ %
20	20.789	1.3300	1.3336	3.9	0.27
22	22.481	1.3300	1.3322	2.4	0.16
24	24.371	1.3300	1.3312	1.8	0.06
26	26.397	1.3300	1.3310	1.9	0.07
28	28.327	1.3300	1.3309	1.6	0.06
30	30.133	1.3300	1.3306	0.6	0.04
32	32.034	1.3300	1.3304	0.2	0.03
34	33.960	1.3300	1.3303	0.2	0.02
36	35.871	1.3300	1.3302	0.6	0.01
38	37.836	1.3300	1.3302	0.8	0.01
40	39.790	1.3300	1.3302	1.0	0.01

### Inhomogeneous case

As shown in the previous section, for inhomogeneous particles the Generalized Airy Theory still posses a harmonic angular shift and an overestimation of the Intensity. Using the same correction function of Eq. 21 and Eq.23 a remarkable improvement of the GAT can be observed. In Figure 11 the comparison between the GLMT, the GAT and the corrected GAT patterns can be observed for a spherical particle with a diameter of 100  $\mu\text{m}$ , possessing a parabolic refractive index gradient ( $m_c=1.332$  &  $m_s=1.333$ ).

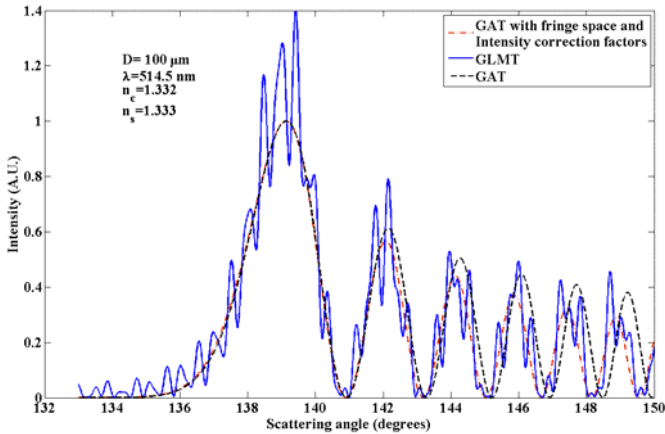


**Figure 11 Comparison between the GLMT (solid line), the GAT (dashed line) and the corrected GAT patterns (dashed dotted line).**

In this paper only a qualitatively comparison of the modified GAT theory and the GLMT one is proposed. A more exhaustive comparison will be proposed in a near future.

### DATA INVERSION ALGORITHM

In this section a data inversion algorithm able to retrieve from experimental Rainbow patterns the particle diameter and its refractive index at core and at surface is shown. This data inversion algorithm is based on the least square fit method using Eqns. 11, 19, 21 and 23 and minimizes the quantity

$$\max |I^{**}(\theta, D, \lambda, m) - \text{Exp}| \quad (24)$$

However the hypothesis of a priori knowledge of the refractive index profile shape has to be made. In this paper we will build the data inversion algorithm assuming a parabolic profile of refractive index. The data inversion algorithm has been used and tested on an n-octane droplet burning in a standard atmosphere.

Some of the refractive indices profiles of such a droplet, during the burning process are shown on Figure 12, the quantity  $\tau = t/t_0$  representing the droplet heating time.

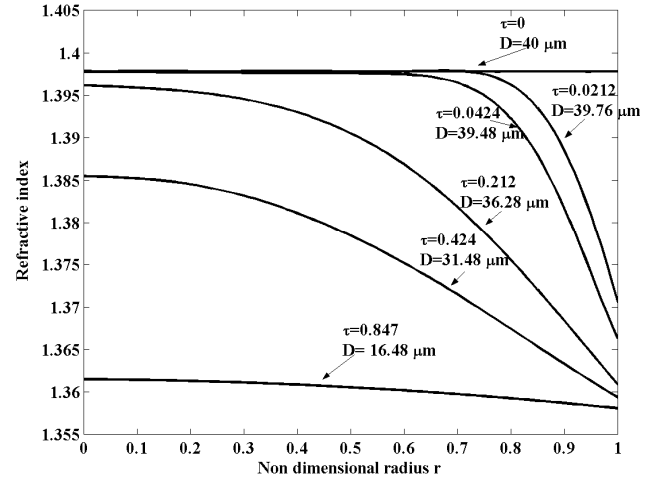


**Figure 12 Internal refractive index profiles of a n-octane droplet burning in a standard atmosphere. The quantity  $\tau$  represents the non-dimensional time  $t/t_0$ , where  $t_0$  is the heating time.**

Starting from these refractive index profiles Gat patterns have been numerically generated and then inverted imposing a parabolic shape of the refractive index gradient.

Figure 13 presents the comparison between the values of refractive index imposed by the profiles of Figure 12 and the corresponding values obtained using the data inversion algorithm.

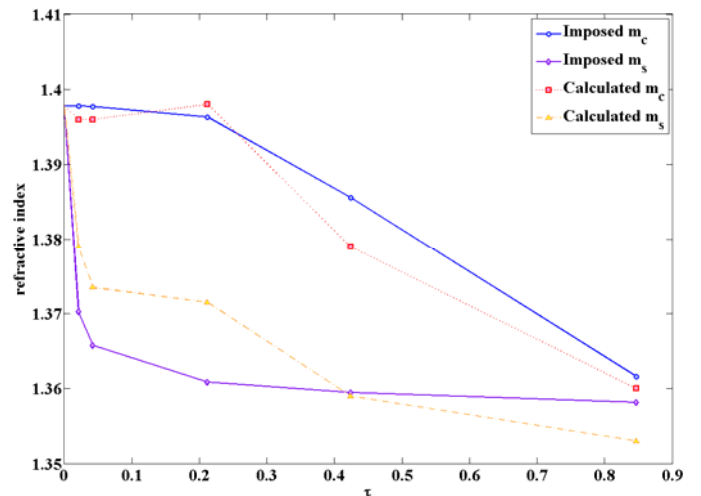


**Figure 13 Comparison between the theoretical refractive index values in the core and at surface of a n-octane droplet burning in standard atmosphere and the values obtained with the old and with the new data inversion algorithm.**



The values corresponding to the core of the droplet are in better agreement than those at surface. The reason why the fitting procedure works better for the core values rather than for the surface ones has to be found in the stronger dependence of the rainbow scattering angle  $\theta_{rg}$  on  $n_c$  than on  $n_s$ .

## CONCLUSIONS

In this paper the discrepancies which exist between the Mie, the Debye and the Airy theory have been evidenced. The use of correction function in the definition of the scattering angle limits these discrepancies which consist in a harmonic shift of the angular position of the rainbow bows and in an overestimation of the rainbow light intensity.

Using these correction functions a significant improvement of the Airy theory for light scattered by small particles is presented both for uniform sphere and for sphere possessing an internal refractive index gradient.

The Airy theory so improved has been used in combination with a data inversion algorithm for evaluation of diameter and refractive index at core and at surface of a non uniform sphere imposing a parabolic shape of the refractive index gradient. Results show how this data inversion algorithm works well for the diameter and the core refractive index evaluation while a larger discrepancy is found for the surface refractive index.

## NOMENCLATURE

Symbol	Quantity	SI Unit
$I, I^*, I^{**}$	Light intensity	A. U
$\theta$	Azimuthal coordinate	Deg.
$\phi$	Polar coordinate	Deg
$r$	Radial coordinate	m.
$k$	Amplitude wave vector	$m^{-1}$
$\lambda$	wavelength	m
$P_n$	Legendre polynomial	
$a_n$	Scattering coefficient	
$b_n$	Scattering coefficient	
$\Psi_n$	Riccati-Bessel function	
$\xi_n$	Riccati-Bessel function	
$a$	Sphere radius	m
$m$	Refractive index	
$p$	Scattering order	
$T^{ij}$	Transmission coefficient	
$R^{ij}$	Reflection coefficient	
$D$	Droplet diameter	M
$\Omega$	Rainbow function	
$z$	Non dimensional scattering angle	
$v$	Spatial coordinate	m
$\tau_{rg}$	Incident rainbow angle	Deg.
$\theta_{rg}$	Scattering rainbow angle	Deg.
$\tilde{r}$	Non-dimensional radius	
$\tilde{r}_m$	Minimal radius	M
$R$	Sphere radius	m
$m_e$	External refractive index	
$m_c$	Core refractive index	
$m_s$	Surface refractive index	
$\Delta m$	Refractive index gradient	
$n_1, t$	Correction function	

$\theta_{min}^{Deb}$	Minima of Debye pattern	Deg.
$\theta_{min}^{Ai}$	Minima of Airy pattern	Deg.
$I^{Deb}$	Intensity of Debye pattern	A. U
$D^{**}$	Diameter	m
$m^{**}$	Refractive index	
$\Delta D^{**}$	Error on diameter calculation	m
$\Delta m^{**}$	Error on refractive index calculation	
$\tau$	Non-dimensional heating time	

## REFERENCES

- [1] G. Mie, "Beitrges zur optic truber medien, speziell kolloidaler metallosungen" Ann. Phys., **25**, 377-452 (1908).
- [2] P. Debye, "Der lichtdruck auf kugeln von beliebigem material", Ann. Phys. 30 57-136 (1909).
- [3] H. M. Nussenzveig, "High-Frequency Scattering by a Transparent Sphere. I. Direct Reflection and Transmission", **10**, Journal of Mathematical Physics 82-164 (1969).
- [4] H. M. Nussenzveig, "High-Frequency Scattering by a Transparent Sphere. II. Theory of Rainbow and glory", **10**, Journal of Mathematical Physics, 125-176 (1969).
- [5] M. R. Vetrano, J. van Beeck and M. Riethmuller, "Generalization of Rainbow Airy theory to non-uniform spheres", Optics Letters, **30**, no. 6, 658-660 (2005).
- [6] J. A. Adams, "The mathematical physics of rainbows and glories", Phys. Rep. 356, 229-365 (2002).
- [7] F. Onofri, G. Gréhan and G. Gouesbet, "Electromagnetic scattering from a multilayered sphere located in an arbitrary beam", Applied Optics, **34**, no 30, 7113-7124 (1995)
- [8] M. R. Vetrano M. R. Vetrano, J. van Beeck and M. Riethmuller, "Generalization of Rainbow Airy theory to non-uniform spheres", Optics Letters, **30**, no. 6, 658-660 (2005).